European Journal of Radiology Open 6 (2019) 169–174

Contents lists available at ScienceDirect

European Journal of Radiology Open

journal homepage: www.elsevier.com/locate/ejro

Evaluation of iron deposition in brain basal ganglia of patients with Parkinson's disease using quantitative susceptibility mapping

Vahid Shahmaei[a], Fariborz Faeghi[a,*], Ahmad Mohammdbeigi[b], Hasan Hashemi[c], Farzad Ashrafi[d]

[a] Radiology Technology Dept., School of Allied Medical Sciences, Shahid Beheshti University of Medical Sciences, Tehran, Iran.
[b] Department of Medical Physics, School of Medicine, Kermanshah University of Medical Sciences, Kermanshah, Iran.
[c] Advanced Diagnostic and Interventional Radiology Research Center (ADIR), Tehran University of Medical Sciences, Tehran, Iran.
[d] Functional Neurosurgery Research Center, Shahid Beheshti University of Medical Sciences, Tehran, Iran.

ARTICLE INFO

Keywords:
Quantitative susceptibility mapping
Parkinson
Basal ganglia
Iron deposition
Magnetic resonance imaging

ABSTRACT

Aim of the study: Parkinson's disease is associated with iron deposition in the brain. The QSM (quantitative susceptibility mapping) is more sensitive than T2-weighted imaging, T2* and R2. Few studies have been used QSM to evaluate the iron in the basal ganglia of patients with Parkinson's disease. Our aim was to evaluate the iron deposition in the basal ganglia using QSM and determination of diagnostic value of this method and evaluation of the association between disease stage with QSM and age with QSM in all nuclei, separately.

Materials and methods: Thirty patients were tested using Hoehn and Yahr test in three different stages. Fifteen healthy subjects were considered as control group. MRI sequences were performed using SIEMENS 3 T scanner.The Signal Processing in NMR software was used to process and analyze the images. The QSM in every of the basal ganglia was measured separately.

Results: There was a significant difference for QSM in the Subtania Nigera, Red Nucleus, Thalamic Nucleus and Globus Pallidus nucleus between two groups. The relationship between disease stage with QSM was significant in Subtania Nigera, Red Nucleus, and Globus Pallidus nucleus. The QSM values had a significant association with disease stage in all nuclei. The results showed that QSM has a higher accuracy in Subtania Nigera, Globus Pallidus, Red Nucleus and Thalamic Nucleus, respectively.

Conclusions: Using QSM in Red Nucleus, Subtania Nigera, and Globus Pallidus nuclei can help diagnosis and staging the patients with Parkinson's disease. In future, studies with emphasis on the disease stage can be helpful in evaluation the different parts of these three nuclei.

1. Introduction

Measurement the iron deposition in brain can explain pathophysiological interactions in the patient's brain [1]. Studies have shown that increased amount of iron is associated with diseases such as multiple sclerosis [2], Alzheimer's disease [3], and Parkinson [4]. Parkinson's disease is the most common malignant neurological disorder after Alzheimer's disease. Iron as the most frequent metal among the transmitter metals in the brain plays an important role in many cellular processes of the cell, including oxygen and electron transport, brain metabolism, myelin production, and dopamine production [5,6]. Parkinson's disease is a chronic and progressive disease in which dopaminergic cells die in the Substania nigera (SN) of the brain and body movements become irregular in the absence of dopamine. Dopamine works as a neurotransmitter mediator in most of brain regions, especially in the dopaminergic pathway from the SN to the caudate and putamen nuclei [7]. Many of observed symptoms in Parkinson's disease are the result of defect in the normal inhibition of basal ganglia, while it can be justifiable considering that the basal ganglia regulate the initiation of motion activities [8]. Studies have shown that ferritin and hemosiderin can be detected by MRI techniques among three different iron storage molecules (transferrin, ferritin, and hemosiderin) in the body. However, transferrin can't be measured through MRI due to low distribution and low concentrations [1]. Many studies have shown that some MRI sequences such as Quantitative Susceptibility Mapping (QSM), T2-weighted imaging, T2*, and R2* mapping can measure the amount of iron deposition in the brain as a biomarker for prognostic the disease and help diagnosis of the disease more accurately [9]. Although

Abbreviations: QSM, Quantitative Susceptibility Mapping; SN, Subtania Nigera; RN, Red Nucleus; GP, Globus Pallidus; PN, Putamen Nucleus; ThN, Thalamic Nucleus; GpN, Globus Pallidus; CN, Caudate Nucleus; PD, Parkinson's disease

* Corresponding author.
E-mail address: f_faeghi@sbmu.ac.ir (F. Faeghi).

https://doi.org/10.1016/j.ejro.2019.04.005
Received 16 January 2019; Received in revised form 15 April 2019; Accepted 16 April 2019
Available online 29 April 2019

research have shown that the R2* method is more sensitive than T2-weighted imaging and T2 *; however, it is still not considered as an appropriate sequence due to the dependence to the magnetic field strength, the presence of blooming artifact that increases with increasing TE, and the lack of relationship with iron concentrations [10]. The QSM (gradient-echo imaging sequence) is a more appropriate sequence than other sequences due to the lack of high probability and higher sensitivity [3,7,11]. As regards that few studies have been conducted using QSM and they were not in all nuclei, different results have been reported, in this study the iron deposition in the Red, Sub substantia nigra, Caudate, Globus Pallidus, Putamen, and Thalamus nuclei of patients with Parkinson's disease was investigated using the quantitative susceptibility mapping.

2. Materials and methods

2.1. Patients and moral confirmations

A total of 30 patients (18 males and 12 females) with Parkinson's disease and 15 healthy subjects (9 males and 6 females) were included the study. Informed consent was obtained from all individual participants included in the study accordance to the supervision of the ethics committee of Shahid Beheshti University of Medical Sciences, Tehran, Iran. Patients were selected from Parkinson's Clinic of Shohada-e-Tajrish Hospital and Neurology Clinic of Imam Khomeini Hospital from September 2017 to July 2018. All subjects were documented by a neurologist with 10 years' experience using the Hoehn and Yahr scale in 0 (healthy), 1, 2 and 3 stages (25). Patients who had pace maker or other electrical implants as well as those with mental, neurological and infectious diseases were excluded.

2.2. MRI parameters and examination method

The imaging was carried out using the 3 T (Tim Trio Siemens Healthcare, Erlangen, Germany) of Imam Khomeini Hospital.A 32-channel coil specialized for Neuroimaging research was also used. In this study, FSE T2 AX, FSE T2 TIRM DARK, FLUID FSE T1 AX, FSE T2 SAG and FSE T2 – COR sequences were evaluated to investigate other diseases. The QSM specialized images have intrinsically low resolution, and to enhance their resolution T1-weighted 3D gradient-echo 3D images (3D T1 MP-RAGE) is used for overlaying on MP-RAGE images. This step was done to increase the accuracy of determining the ROI of different nuclei. The QSM special sequences were used to evaluate the Parkinson's disease with this specification: TE = 4–41.8 ms, TR = 38 ms, FOV = 256 mm, TR = 38 ms, Matrix size = 256 * 256, FA = 15°, Slice thickness = 1.5 mm, bandwidth = 704 Hz / pixel, and the acquisition time of 9 min.

2.3. Image processing and analysis

The obtained images in DICOM format were transferred to Signal Processing in NMR (SPIN) [12] software for processing. In this study 3D GRE T2* images were analyzed using SPIN software. In first, the skull bone is removed using the BET command to study only the magnetic effects of brain tissue. We eliminate a sharp background noise using a high pass filter and a SHARP filter. In the next, we corrected the out of field non-uniformity of voxels that affect the ROI using the inverse filter algorithm. After these steps, we extract the final QSM images in the brain's magnetic susceptibility maps in the DICOM format. Eventually, the QSM sequence images were overlayed on MP-RAGE images for increasing the resolution of the images to determining ROI more precisely. The ROI was positioned in every slice that cover the largest and most complete anatomical region [Fig. 1a and b]. Then mean QSM values were measured in each determined ROI of the bilateral Red, Substantia Nigra, Caudate, Globus Pallidus, Putamen, and Thalamus nuclei. This step was performed with the help of a radiologist with the experience of 25 years.

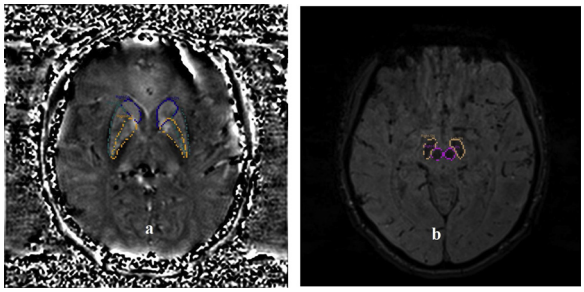

Fig. 1. a) Representative slice show the determined ROI for CN(blue color), PUT(yellow color) and GP(green color), b) the determined ROI for RN(purple color), SN(yellow color) in SPIN software. The ROIs determined manually by the educated radiologic thchnologist.

2.4. Statistical analysis

The SPSS 21.0 software is used for statistical analysis in this study. Initially, the K-S test was examined for assessing the normality of QSM values. Parametric *t*-test and Mann-Whitney test were used to comparison QSM values between control and patient groups. Regarding the data abnormality, Spearman Correlation Coefficient was used in each of the nuclei to investigate the relationship between QSM and stage. Also, ROC curve (receiver operating characteristic) used to determine the sensitivity, specificity and accuracy based on QSM. In all tests, the confidence interval was 0.95 and the significance level was 0.05.

3. Results

The mean age in the control group was 64.9 ± 9.2 and in the case group was 66.2 ± 8.5. Subjects in both control and PD group were consistent in terms of age and did not have any significant difference (P-value = 0.59). The frequency and frequency percentage of subjects are summarized in Table 1 for different stage of disease.

3.1. Comparison of QSM values between control and patient groups

The mean ± standard deviation and P-value for QSM between the control and PD groups, differentiated by the nucleus, are shown in Table 2. For QSM, there was a significant difference between the control group and the PD group for all of the nuclei except for the PN and CN.

3.2. Correlation coefficients

Correlation between QSM values with age and QSM with stage calculated using Spearman correlation coefficient and is shown in table [Tables 3 and 4].

The results showed the correlation between QSM with age was not significant in any of the nuclei [Table 3]. However, the correlation of stage with QSM was significant in SN, RN and GP nuclei [Table 4].

Table 1
Frequency and percent of subjects in different stages.

	Stage	Frequency	Percent
Control	0	15	33.3
PD	1	8	17.8
	2	11	24.4
	3	11	24.4
Total	–	45	100.0

Table 2
Comparison QSM between PD and control group.

	QSM(ppm)		
	Control	PD	P
SN	0.146 ± 0.026	0.239 ± 0.021	< **0.001**
RN	0.173 ± 0.009	0.201 ± 0.018	< **0.001**
PN	0.163 ± 0.032	0.152 ± 0.022	**0.160**
GpN	0.178 ± 0.027	0.247 ± 0.028	< **0.001**
ThN	0.108 ± 0.008	0.119 ± 0.012	**0.005**
CN	0.155 ± 0.011	0.153 ± 0.027	**0.193**

Table 3
Correlation of QSM with age using Spearman Correlation Coefficient.

Nucleus	P-value	R
SN	0.220	0.187
RN	0.342	0.145
PN	0.211	−0.190
GpN	0.213	0.203
ThN	0.604	0.079
CN	0.144	0.221

Table 4
Correlation between QSM and stage using Spearman Correlation Coefficient.

Nucleus	P-value	R
SN	< 0.001	0.751
RN	< 0.001	0.538
PN	0.595	−0.082
GpN	< 0.001	0.751
ThN	0.167	0.209
CN	0.283	0.164

3.3. Estimation of the diagnostic value of QSM

The sensitivity, specificity, and accuracy of QSM values are shown in every nucleus by percentage, in Table 5. Also, the ROC curves is shown in Figs. 2–5 for all nuclei, separately. The sensitivity was higher in SN, GP, RN and ThN, respectively. However, the specificity was higher in RN, SN, GP and ThN respectively. Also, the accuracy was higher in SN, GP, RN and ThN, respectively.

4. Discussion

In this study, we compared QSM values among PD and healthy subjects to examine the ability of these two variables to diagnosing and staging.

In general, the highest changes in QSM have been observed in SN nucleus [Table 2]. A significant difference founded for QSM values between the PD and control groups in the SN nucleus, which was consistent with the results of all previous studies performed with R2* sequences, except for the two studies of Kosta and Bartzokis [13,14], also was consistent with Postmortem and SWI studies, except for three studies of Du, Graham and Wypijewska [11,15,16]. The QSM-based studies also confirm these results and show an increase in the iron deposition rate in patients compared to healthy subjects [3,4,7,17]. Thus, our study showed the QSM is an appropriate method to diagnosis of patients with PD in SN as well as most previous studies that have been demonstrated. However, Sofic and Martin examined the SN nucleus in four distinct anatomical parts and indicated that the QSM changes were not necessarily related to all parts of the core, and in some parts like SNr, there was no difference between the control group and the patient group. Therefore, more studies are required using the QSM to obtain more accurate information in different parts of the SN separately, also using devices with magnetic field stronger than 3 T, which have more accuracy for measurement of QSM [18,19].

Table 5
Sensitivity, specificity and accuracy values of QSM determined for every nucleus using ROC curve.

Nucleus	Sensitivity	Specificity	Accuracy
SN	100.0	93.0	98.0
RN	80.0	100.0	86.7
GpN	90.0	86.7	88.9
ThN	73.3	66.7	71.1

For RN nucleus, a significant difference founded for QSM values between two groups [Table 2]. Jian-Yong Wang et al. published a meta-analysis for assessment R2* and SWI studies, and their results were consistent with our results [20]. Wang et al. also stated, there is no difference in iron deposition between healthy and patient groups in two studies [7,21] out of twelve, that included in their meta-analysis study. They mentioned that reason of this phenomenon was low staging of patients in these two studies. The Strong correlation between stage and QSM in our study also confirm it. This can confirm the results of Guan et al. [22] study, which obtained increasing QSM values in the patient group for high stages. As regards increasing the Iron deposition in RN nucleus depends on disease staging. Future studies for the RN nucleus with focusing on disease stage and the QSM, which has a higher accuracy than R2* and SWI can be helpful.

There was no difference between control and PD group in the PN [Table 2]. Although this results was in contrast to the results of Wang et al. study, however as regards only one postmortem study [23] had shown positive results in increasing the iron deposition in this nucleus, and another studies are required to achieve more accurate results [24–28]. The result of Wang et al. for SWI studies also confirms the results of our study. However, there wasn't any QSM study that show increasing QSM in PD patients and all previous studies [3,4,7] have reported non changing the iron deposition in PD patients. The reason for this is the difference in the used sequence and the difference in ROI (7). However, PN is considered as an external nucleus and QSM is more accurate in internal basal nuclei, thus it can be stated that QSM cannot be as accurate as R2* in PN. It has been proved by Postmortem studies, calcium and magnesium deposition in the PN increases with increasing age (20); Therefore, low accuracy of QSM to the iron deposition in PN can be due to increasing the effect of other paramagnetic materials such as magnesium. The weak correlation of staging with QSM also indicates PN can't be an appropriate choice for evaluating PD using QSM.

For GP nucleus, the Wang et al. study showed that among SWI, R2* and postmortem just SWI approved the iron deposition increases in GP nucleus of PD patients. Our study demonstrated there is a significant difference in the amount of iron and QSM that is consistent with the study of Langkammer et al. and Guan et al., but was contrast with two other studies (4, 7). Thus, it seems the conclusion about GP nucleus as a choice for diagnosis of patient with PD is complicated and needs more studies using stronger magnetic fields and larger sample size.

For ThN, there was a significant difference in QSM values between the PD group and control group [Table 2], which is in contrast to the SWI and R2* studies (28–32). The study of Langkammer et al. using the QSM is in agreement with this study. ThN had the lowest QSM values which is consistent with the results of Guan et al study. Low values of QSM in ThN and its lack of correlation with disease stage [Table 4] indicate that this technique is not very helpful in this nucleus. The low accuracy of this method for diagnosis of PD patients also confirms this claim [Table 5].

For CN, as well as in the PN, there was no difference in QSM values between the control group and the PD group [Table 2]. This result is consistent with the previous studies (3,7).

In this study, we didn't find any association between QSM and age in any of nuclei [Table 3]. However, it has been proved that with increasing age iron deposition in the brain increases in normal people.

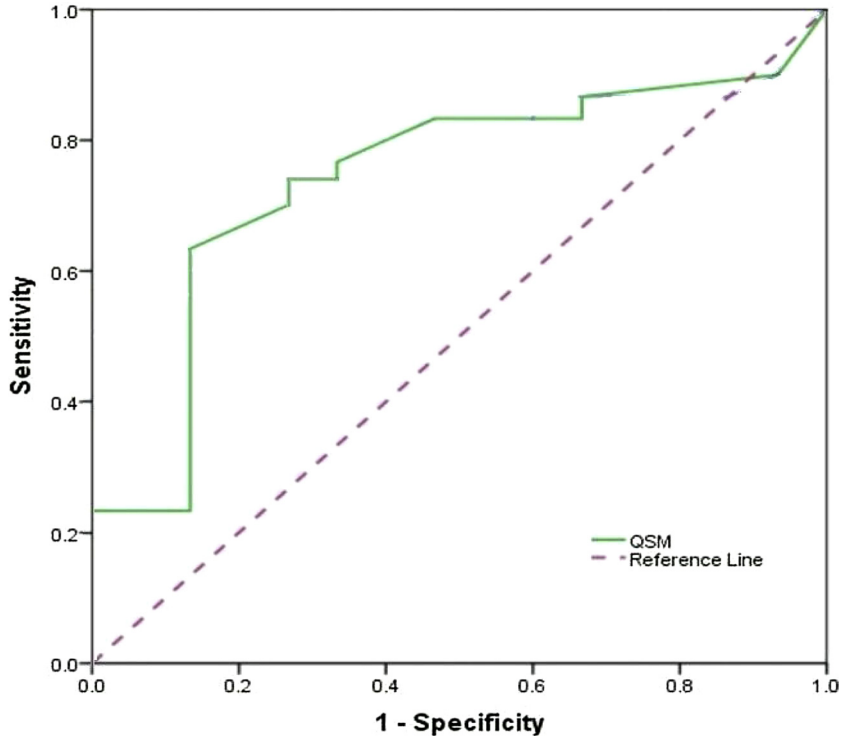

Fig. 2. ROC Curve analysis of QSM between Parkinson's disease and healthy subjects in Thalamus Nucleus showed the 73.3, 66.7 and 71.1 for sensitivity, specificity and accuracy, respectively.

Due to the small sample size in control group, we did not asses the correlation of age with QSM in the control and patient groups separately, which this may be one of the reasons for differences of our results with other studies.

Our study demonstrated the correlation between QSM with disease stage was strong in GP, SN, and RN nuclei [Table 4], which it was

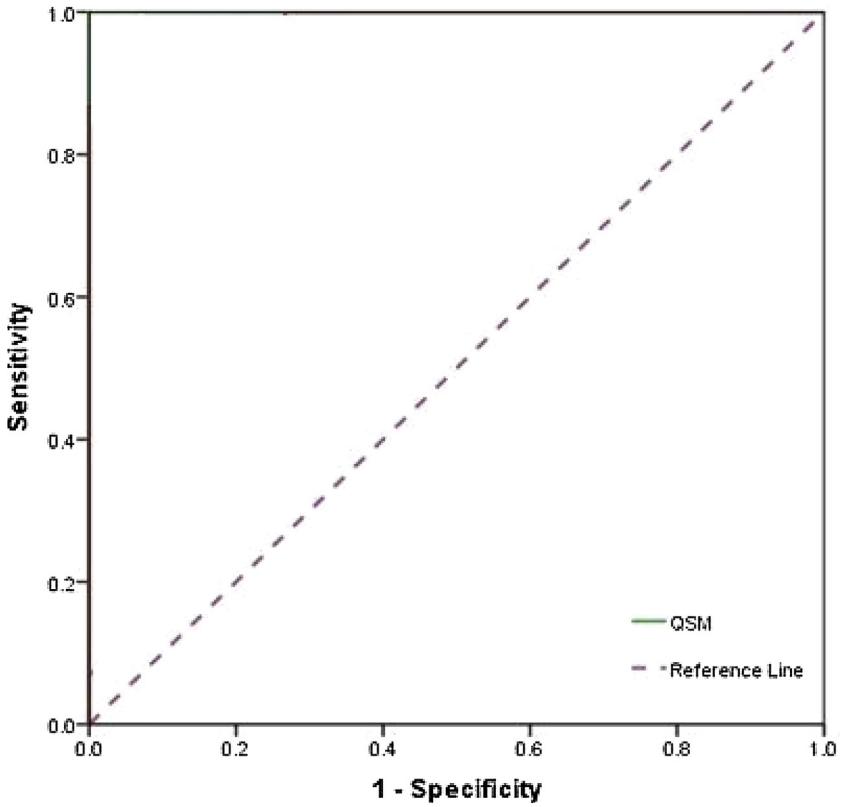

Fig. 3. ROC Curve analysis of QSM between Parkinson's disease and healthy subjects in SN Nucleus showed the 100.0, 93.0 and 98.0 for sensitivity, specificity and accuracy, respectively.

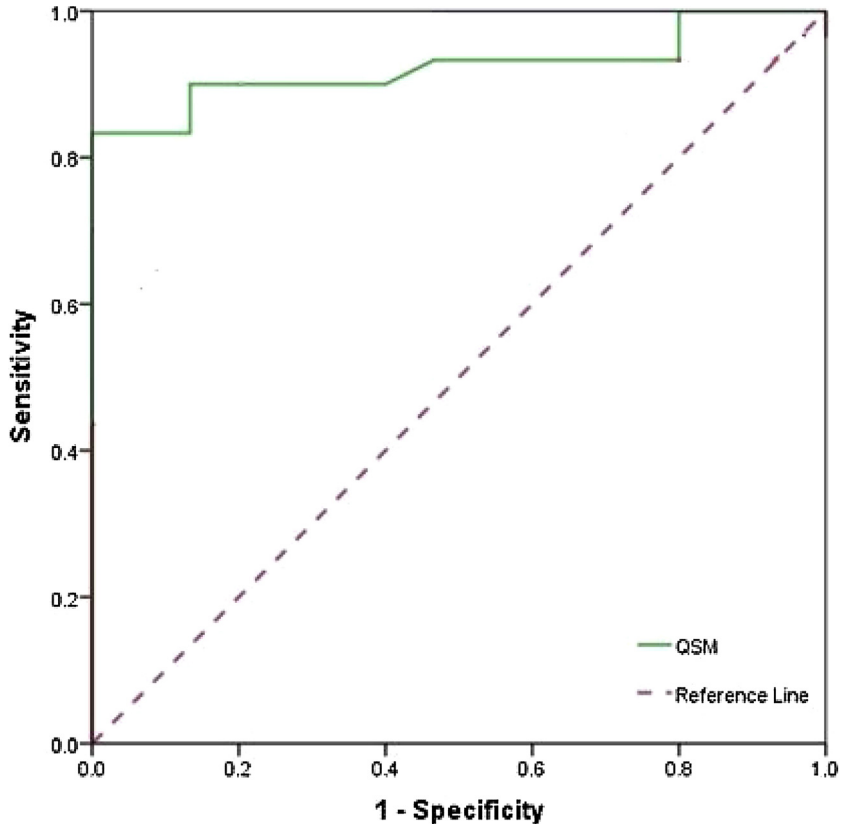

Fig. 4. ROC Curve analysis of QSM between Parkinson's disease and healthy subjects in RN Nucleus showed the 80.0, 100.0 and 86.7 for sensitivity, specificity and accuracy, respectively.

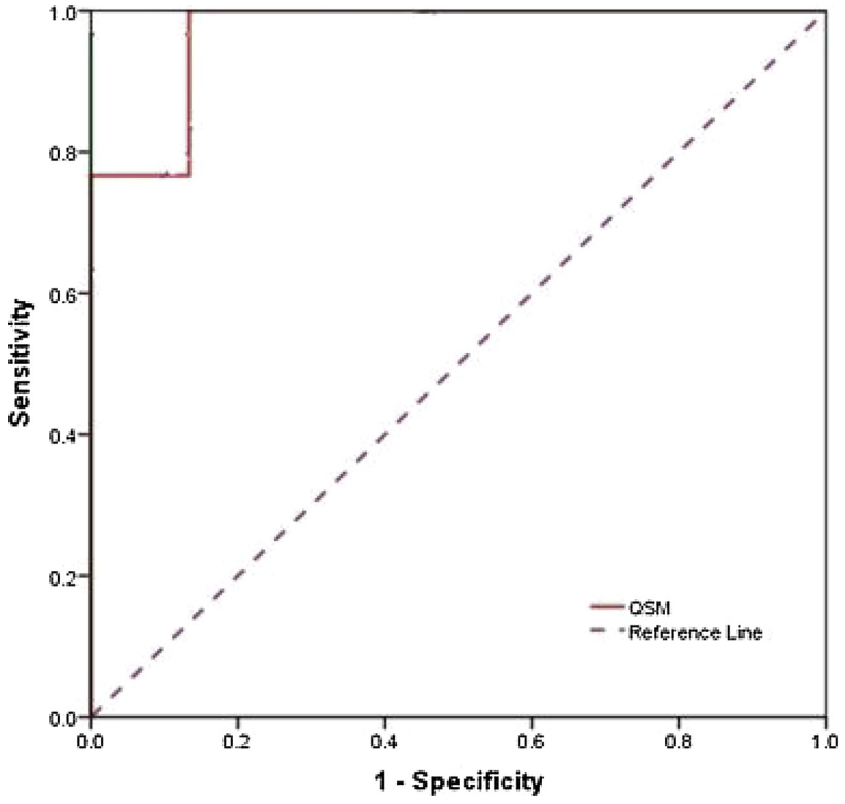

Fig. 5. ROC Curve analysis of QSM between Parkinson's disease and healthy subjects in Gp Nucleus showed the 90.0, 86.7 and 88.9 for sensitivity, specificity and accuracy, respectively.

weaker for the RN. Du et al. and Zhang et al. showed there is a correlation between QSM and UPDRS-II in the SN nucleus. Langkammer et al. showed there is a correlation between the H & Y test and QSM in SN and GP nuclei for patients who had a longer period of disease. However, the GP nucleus did not show a relationship between QSM and the H & Y test over a shorter period of time. Given that 70% of our patients were in stages 2 and 3 [Table 1], and QSM had also a strong correlation with the disease stage [Table 4], our results can be justifiable for the GP nucleus.

Our study had several limitations: first, we considered ROI in this study only in one slice. In future, studies with volumetric measurements can give more accurate results. Second, Considering the SN nucleus into SNr and SNc sections and assessing everyone separately can give more precise results, in contrast of whole evaluating the SN. Third, this technique cannot detect different types of iron or neurons iron from microglia iron and is even influenced by susceptibility of tissues, therefore histopathological studies along with QSM studies will be very helpful.

5. Conclusions

In summary, using QSM in RN, SN, and GP nuclei can help diagnosis and staging the patients with PD especially in SN. In future, studies with emphasis on the disease stage can be helpful in evaluation the different parts of these three nuclei.

Conflict of interest

All authors declare that they have no conflict of interest.

Acknowledgements

This work was performed in partial fulfillment of the requirements for MSc of Medical Imaging (MRI) of Vahid Shahmaei in School of allied Medical Sciences, Shahid Beheshti University of Medical Sciences. The authors would like to thank the staff of Imam Khomeini Hospital..

References

[1] E.M. Haacke, N.Y. Cheng, M.J. House, Q. Liu, J. Neelavalli, R.J. Ogg, et al., Imaging iron stores in the brain using magnetic resonance imaging, Magn. Reson. Imaging 23 (1) (2005) 1–25.
[2] C.A. Habib, M. Liu, N. Bawany, J. Garbern, I. Krumbein, H.J. Mentzel, et al., Assessing abnormal iron content in the deep gray matter of patients with multiple sclerosis versus healthy controls, AJNR Am. J. Neuroradiol. 33 (2) (2012) 252–258.
[3] C. Langkammer, S. Ropele, L. Pirpamer, F. Fazekas, R. Schmidt, MRI for iron mapping in Alzheimer's disease, Neurodegener. Dis. 13 (2–3) (2014) 189–191.
[4] J.H. Barbosa, A.C. Santos, V. Tumas, M. Liu, W. Zheng, E.M. Haacke, et al., Quantifying brain iron deposition in patients with Parkinson's disease using quantitative susceptibility mapping, R2 and R2, Magn. Reson. Imaging 33 (5) (2015) 559–565.
[5] D.J. Hare, P.A. Adlard, P.A. Doble, D.I. Finkelstein, Metallobiology of 1-methyl-4-phenyl-1,2,3,6-tetrahydropyridine neurotoxicity, Metallomics 5 (2) (2013) 91–109.
[6] J. Stankiewicz, S.S. Panter, M. Neema, A. Arora, C.E. Batt, R. Bakshi, Iron in chronic brain disorders: imaging and neurotherapeutic implications, Neurotherapeutics 4 (3) (2007) 371–386.
[7] Y. Murakami, S. Kakeda, K. Watanabe, I. Ueda, A. Ogasawara, J. Moriya, et al., Usefulness of quantitative susceptibility mapping for the diagnosis of Parkinson disease, AJNR Am. J. Neuroradiol. 36 (6) (2015) 1102–1108.
[8] J.E. Ahlskog, Parkinson's disease: is the initial treatment established? Curr. Neurol. Neurosci. Rep. 3 (4) (2003) 289–295.
[9] C. Liu, W. Li, G.A. Johnson, B. Wu, High-field (9.4 T) MRI of brain dysmyelination by quantitative mapping of magnetic susceptibility, Neuroimage 56 (3) (2011) 930–938.
[10] T.L. Davis, K.K. Kwong, R.M. Weisskoff, B.R. Rosen, Calibrated functional MRI: mapping the dynamics of oxidative metabolism, Proc. Natl. Acad. Sci. U. S. A. 95 (4) (1998) 1834–1839.
[11] G. Du, M.M. Lewis, M. Styner, M.L. Shaffer, S. Sen, Q.X. Yang, et al., Combined R2* and diffusion tensor imaging changes in the substantia nigra in Parkinson's disease, Mov. Disord. 26 (9) (2011) 1627–1632.
[12] E.M. Haacke, M. Ayaz, A. Khan, E.S. Manova, B. Krishnamurthy, L. Gollapalli, et al., Establishing a baseline phase behavior in magnetic resonance imaging to determine normal vs. abnormal iron content in the brain, J. Magn. Reson. Imaging 26 (2) (2007) 256–264.
[13] G. Bartzokis, J.L. Cummings, C.H. Markham, P.Z. Marmarelis, L.J. Treciokas, T.A. Tishler, et al., MRI evaluation of brain iron in earlier- and later-onset Parkinson's disease and normal subjects, Magn. Reson. Imaging 17 (2) (1999) 213–222.
[14] P. Kosta, M.I. Argyropoulou, S. Markoula, S. Konitsiotis, MRI evaluation of the basal ganglia size and iron content in patients with Parkinson's disease, J. Neurol. 253 (1) (2006) 26–32.
[15] J.M. Graham, M.N. Paley, R.A. Grunewald, N. Hoggard, P.D. Griffiths, Brain iron deposition in Parkinson's disease imaged using the PRIME magnetic resonance sequence, Brain 123 (Pt 12) (2000) 2423–2431.
[16] A. Wypijewska, J. Galazka-Friedman, E.R. Bauminger, Z.K. Wszolek, K.J. Schweitzer, D.W. Dickson, et al., Iron and reactive oxygen species activity in parkinsonian substantia nigra, Parkinsonism Relat. Disord. 16 (5) (2010) 329–333.
[17] E. Sofic, W. Paulus, K. Jellinger, P. Riederer, M.B. Youdim, Selective increase of iron in substantia nigra zona compacta of parkinsonian brains, J. Neurochem. 56 (3) (1991) 978–982.
[18] M. Cosottini, D. Frosini, I. Pesaresi, G. Donatelli, P. Cecchi, M. Costagli, et al., Comparison of 3T and 7T susceptibility-weighted angiography of the substantia nigra in diagnosing Parkinson disease, AJNR Am. J. Neuroradiol. 36 (3) (2015) 461–466.
[19] A.I. Blazejewska, S.T. Schwarz, A. Pitiot, M.C. Stephenson, J. Lowe, N. Bajaj, et al., Visualization of nigrosome 1 and its loss in PD: pathoanatomical correlation and in vivo 7 T MRI, Neurology 81 (6) (2013) 534–540.
[20] J.Y. Wang, Q.Q. Zhuang, L.B. Zhu, H. Zhu, T. Li, R. Li, et al., Meta-analysis of brain iron levels of Parkinson's disease patients determined by postmortem and MRI measurements, Sci. Rep. 6 (2016) 36669.
[21] S.F. Wu, Z.F. Zhu, Y. Kong, H.P. Zhang, G.Q. Zhou, Q.T. Jiang, et al., Assessment of cerebral iron content in patients with Parkinson's disease by the susceptibility-weighted MRI, Eur. Rev. Med. Pharmacol. Sci. 18 (18) (2014) 2605–2608.
[22] X. Guan, M. Xuan, Q. Gu, P. Huang, C. Liu, N. Wang, et al., Regionally progressive accumulation of iron in Parkinson's disease as measured by quantitative susceptibility mapping, NMR Biomed. 30 (4) (2017).
[23] J.C. Chen, P.A. Hardy, W. Kucharczyk, M. Clauberg, J.G. Joshi, A. Vourlas, et al., MR of human postmortem brain tissue: correlative study between T2 and assays of iron and ferritin in Parkinson and Huntington disease, AJNR Am. J. Neuroradiol. 14 (2) (1993) 275–281.
[24] D.T. Dexter, F.R. Wells, A.J. Lees, F. Agid, Y. Agid, P. Jenner, et al., Increased nigral iron content and alterations in other metal ions occurring in brain in Parkinson's disease, J. Neurochem. 52 (6) (1989) 1830–1836.
[25] P. Riederer, E. Sofic, W.D. Rausch, B. Schmidt, G.P. Reynolds, K. Jellinger, et al., Transition metals, ferritin, glutathione, and ascorbic acid in parkinsonian brains, J. Neurochem. 52 (2) (1989) 515–520.
[26] P.D. Griffiths, A.R. Crossman, Distribution of iron in the basal ganglia and neocortex in postmortem tissue in Parkinson's disease and Alzheimer's disease, Dementia 4 (2) (1993) 61–65.
[27] E. Sofic, P. Riederer, H. Heinsen, H. Beckmann, G.P. Reynolds, G. Hebenstreit, et al., Increased iron (III) and total iron content in post mortem substantia nigra of parkinsonian brain, J. Neural Transm. 74 (3) (1988) 199–205.
[28] D.A. Loeffler, J.R. Connor, P.L. Juneau, B.S. Snyder, L. Kanaley, A.J. DeMaggio, et al., Transferrin and iron in normal, Alzheimer's disease, and Parkinson's disease brain regions, J. Neurochem. 65 (2) (1995) 710–724.